Trends Phytochem. Res. 5(4) 2021 210-217

Trends in Phytochemical Research (TPR)

Journal Homepage: http://tpr.iau-shahrood.ac.ir

Original Research Article

Phytochemical studies of *Tetrataenium nephrophyllum* and anti-acetylcholinesterase activities

Mehdi Abbasi[1], Marzie Omrani[1], Leila Raiatparvar Malieki[1], Ali Sonboli[2], And Samad Nejad Ebrahimi[1*]

[1]Department of Phytochemistry, Medicinal Plants and Drugs Research Institute, Shahid Beheshti University, Evin, Tehran, Iran
[2]Department of Biology, Medicinal Plants and Drugs Research Institute, Shahid Beheshti University, Evin, Tehran, Iran

ABSTRACT

Tetrataenium nephrophyllum belonging to the Apiaceae family grows widely in the West Azerbaijan province of Northwestern Iran. It is an aromatic plant that has been used as food spices by local people. In this research work, the phytochemical composition of *n*-hexane extract from the aerial parts of this plant has been investigated. The fractionation of the *n*-hexane extract by normal phase column chromatography resulted in the isolation, purification, and identification of five compounds. The structural elucidation was accomplished by extensive spectroscopic methods, including 1D and 2D NMR experiments (^{1}H-NMR, H-H-COSY, HSQC, HMBC, and NOESY) as well as ESI-MS analysis. The isolated compounds were 5-geranyloxycoumarin (**1**), isobergapten (**2**), pimpinellin (**3**), β-sitosterol (**4**) and dammara-20,23-dien-3β,25-diol. The acetylcholinesterase inhibitory activity of the isolated compound was evaluated by experimental and molecular docking methods. Compound 3 showed the best acetylcholinesterase inhibitory with an IC_{50} value of 0.208 μM and docking score of -7.5 kcal/mol.

ARTICLE HISTORY

Received: 07 December 2021
Revised: 15 December 2021
Accepted: 22 December 2021
ePublished: 27 December 2021

KEYWORDS

Apiaceae
Coumarin
Molecular docking
Phytochemical profiling

1. Introduction

Alzheimer's disease (AD), a neurodegenerative illness characterized by a progressive decline in cognitive function, is the fourth leading cause of death for people over 65 in Western industrial countries (Launer et al., 1999). The principal role of acetylcholinesterase (AChE) is the termination of nerve impulse transmission at the cholinergic synapses by rapid hydrolysis of acetylcholine (AChE). Inhibition of AChE serves as a strategy for Alzheimer's disease (AD) treatment, senile dementia, ataxia, myasthenia gravis, and Parkinson's disease (Brenner, 2000; Choudhary, 2001; Mukherjee et al., 2007). There are only a few synthetic medicines, *e.g.*, tacrine, donepezil, and the natural product-based rivastigmine for treating cognitive dysfunction and memory loss associated with AD (Oh et al., 2004). These compounds have been reported to have adverse effects, including gastrointestinal disturbances and problems associated with bioavailability (Melzer, 1998; Schulz, 2003; Ashrafi et al., 2020; Haghighatseir et al., 2020), which necessitates the interest in finding better AChE inhibitors from natural resources.

The genus *Tetrataenium* (DC.) Manden. (Syn.: Heracleum L. sect. *Tetrataenium* DC.) as a member of the Peucedaneae tribe and Apiaceae family is represented in the Flora Iranica area by five perennial species, two of which grow in Iran. *T. lasiopetalum* (Boiss.) Manden. (Syn.: *Heracleum lasiopetalum* Boiss.) is distributed in southwestern parts of Iran, while *T. nephrophyllum* (Leute) Manden., an endemic species to Iran, occurs in western and northwestern provinces (Azerbaijan, Kurdestan, and Lorestan) (Rechinger KH. 1982). In traditional medicine, leaves and fruits of *Heracleum* and *Tetrataenium* species are used as antiseptic, carminative, digestive, a flavoring agent and spice for foods. To the best of our knowledge, there are no phytochemical investigations except essential oil analysis of *T.*

✉ Corresponding author: Samad Nejad Ebrahimi
Tel.: +98 21 29904052; Fax: +98 21 22431783
E-mail address: s_ebrahimi@sbu.ac.ir, **doi: 10.30495/tpr.2021.1946692.1232**

nephrophyllum (Sonboli et al., 2007). Therefore, the present study was focused on phytochemical investigation of *T. nephrophyllum*, a native plant of Iran, and the evaluation of acetylcholinesterase inhibitory activity of its *n*-hexane extract and isolated compounds using the experimental and molecular modeling approach.

2. Experimental

2.1. Reagents and materials

Silica gel (70-230 mesh) was used for column chromatography (CC) and precoated silica gel F254 (20 cm × 20 cm) plates for TLC, both supplied by Merck. NMR spectra were recorded at a target temperature of 18 °C on a Bruker Avance III 500 MHz spectrometer operating at 500.13 MHz for ^{1}H and 125.77 MHz for ^{13}C with TMS as an internal standard. Spectra were analyzed using Bruker TopSpin 3.1 software. $CDCl_3$ for NMR, acetylcholinesterase (AChE), and acetylthiocholin iodide (ATCI) were purchased from Armar Chemicals, Sigma (Germany), and Merck (Germany), respectively. Moreover, 5,5'-dithiobis-(2-nitrobenzoic acid) (DTNB) and other chemicals and solvents were provided from Merck (Germany).

2.2. Plant material

The aerial parts of *T. nephrophyllum*, including leaves and stems, were collected West Azarbaijan, Takab, Iran, in September 2015. Dr. Ali Sonboli from the Department of Biology, Medicinal Plants and Drug Research Institute (MPDRI), Shahid Beheshti University, Tehran, Iran, botanically identified the plant materials and a voucher specimen (MPH-908) was deposited at the herbarium of MPDRI.

2.3. Extraction and isolation

Dried aerial parts (800 g), including leaves and stems, of *T. nephrophyllum* were powdered and extracted five times for 72 h with 3 L of *n*-hexane at room temperature. After evaporation to dryness under reduced pressure, 18 g of dry extract was obtained. A portion (17 g) of *n*-hexane extract was fractionated on a silica gel column (5 × 40 cm, mesh 70-230) eluted with mixtures of *n*-hexane-EtOAc (100:0, 90:10, 80:20, 70:30, 50:50, 20:80, 0:100, each fraction was 250 mL), followed by increasing ratio of MeOH (up to 100%) in EtOAc (90 :10, 80:20, 70:30, 50:50, 0:100; 250 mL of each) to give 20 fractions (F1-F20). The flow rate was nearly 15 mL/min. The combination of fractions was based on TLC patterns (bands were detected on TLC under UV or by heating after spraying with 5% of phosphomolybdic acid in EtOH). Fraction 7 (1.8 g) was subjected to silica gel column chromatography (63-200 µm, 2.5× 60 cm) and eluted with $CHCl_3$-EtOAc to afford fifteen subfractions (F_{7-1}-F_{7-15}). Subfraction F_{7-5} was recrystallized from acetone to obtain compound **1** (2.8 mg > 98% [^{1}H-NMR]). Subfraction F_{7-9} and F_{7-10} was recrystallized from acetone to obtain β-sitosterol (**4**) (30 mg > 98% [^{1}H-NMR]). Subfraction F_{7-6} [2 mg, eluted with $CHCl_3$- EtOAc (95:5)] was separated by silica gel CC (63-200 µm, 0.5 × 10 cm) and *n*-hexane-EtOAc [80:20, 70:30, 50:50, 0:100; 5 mL each], as the mobile phase, than crude crystals were obtained, which were recrystallized from acetone to give **2** (0.74 mg > 98% [^{1}H-NMR], commonly known as isobergapten (**2**). Fraction F9 (1.2 g) was further purified on a silica gel column (2.5 × 30 cm, mesh 230-400) [dichloromethane -EtOAc (9:1) → (0:10)] to afford Twelve subfractions (F_{9-1}-$F_{9-12'}$ 30 mL each). Subfraction F_{9-4} was recrystallized from acetone to obtain **3** (2 mg > 98% [^{1}H-NMR]). Semi-preparative RP-HPLC (ACN in H_2O (60% to 100% ACN in 30 min; flow rate 20 mL/min) of fraction F13 (200 mg) gave **5** (5 mg > 98%).

2.4. Spectroscopic data of isolated compounds

Compound **1** was obtained as a white sediment (2.8 mg). ^{1}H NMR (500 MHz, $CDCl_3$) δ 7.67 (d, *J* = 9.5 Hz, 1H, H-4), 7.40 (d, *J* = 8.6 Hz, 1H, H-8), 6.89 (dd, *J* = 8.6, 2.4 Hz, 1H, H-7), 6.85 (d, *J* = 2.4 Hz, 1H, H-6), 6.27 (d, *J* = 9.5 Hz, 1H, H-3), 5.51 (td, *J* = 6.5, 1.1 Hz, 1H, H-2′), 5.13 (ddd, *J* = 6.7, 5.4, 1.1 Hz, 1H, H-6′), 4.66 (d, *J* = 6.5 Hz, 2H, H-1′), 2.16 (td, *J*=12.1, 6.1, 2H, H-5′), 2.13 (td, 12.1, 6.1, 2H, H-4′), 1.81 (s, 1H, H-3′a), 1.72 (s, 1H, H-7′a), 1.65 (s, 1H, H-8). ESIMS *m/z* $[M + H]^+$= 299 and $[M-H]^-$= 297. The structure was confirmed as it was compared with literature data (Iranshahi et al., 2012)

Compound (**2**)

White sediment (0.74 mg). ^{1}H NMR (500 MHz, $CDCl_3$) δ 7.68 (d, *J* = 9.8 Hz, 1H, H-3), 7.10 (d, *J* = 2.2 Hz, 1H, H-b), 6.56 (d, *J* = 2.2 Hz, 1H, H-a), 6.42 (s, 1H, H-6), 5.83 (d, *J* = 9.8 Hz, 1H, H-4), 3.50 (s, 3H, H-1′). HR-ESIMS *m/z* $[M+H]^+$= 217. The obtained data were compared with literature data to confirm the structure (Ozek et al., 2019).

Compound (**3**)

^{1}H NMR (500 MHz, $CDCl_3$) δ 7.98 (d, *J* = 9.8 Hz, 1H, H-3), 7.57 (d, *J* = 2.1 Hz, 1H, H-b), 6.99 (d, *J* = 2.1 Hz, 1H, H-a), 6.27 (d, *J* = 9.8 Hz, 1H,H-4), 4.06 (s, 3H, H-1′), 3.95 (s, 3H, H-2′). HR-ESIMS *m/z* 246 $[M+H]^+$= 247. According to literature data, this structure was confirmed (Ozek et al., 2019).

Compound (**5**)

^{1}H NMR (500 MHz, $CDCl_3$) δ 5.58 (m, 1H, H-23), 5.72 (dt, *J* = 16.7 1H, H-24), 4.79 and 4.71 (1H, s, H-21), 3.14 (dd, *J* = 10.6 Hz, 1H, H-3), 2.57 (d, *J*=7 Hz, 2H, H-22), 2.11 (m, 1H, H-17), 1.8 and 1.32 (m, 1H, H-29), 1.8 and 1.03 (m, 1H, H-12), 1.74 and 1.19 (m, 1H, H-15), 1.63 and 1.43 (m, 1H, H-6), 1.62 and 0.86 (m, 1H, H-1), 1.52 and 1.49 (m, 1H, H-2), 1.48 and 1.19 (m, 1H, H-7), 1.42 and 1.11 (m, 1H, H-21), 1.58 (m, 1H, H-13), 1.36 (s, 3H, H-26 overlapped, H-27), 0.9 (s, 3H, H-30), 0.89 (s, 3H, H-18 overlapped H-28), 0.77 (s, 3H, H-19), 0.68 (s, 3H, H-29), 0.63 (dd, *J* = 12.5 Hz , *J* = 1.3 Hz, 1H, H-5). HR-ESIMS *m/z* $[M+H]^+$= 425. This structure was confirmed compared with literature data (Révész et al., 1999).

2.5. Acetylcholinesterase inhibitor assay

AChE inhibitory activities were determined using the general method of Ellman (Ellman et al., 1961; Abbas-Mohammadi et al., 2020). The samples were dissolved in methanol (3000 µg/mL). 125 µL of DTNB (3 mM), 25 µL of ATCI (15 mM), 50 µL of phosphate buffer (pH 8), and 25 µL of the sample dissolved in methanol were added to wells of 96-well plates. The absorbance was recorded at 405 nm every 13 s for 65 s. 25 µL of 0.22 U/mL of AChE enzyme was then added and the absorbance was again measured every 13 s for 104 s using a TECAN ELISA reader at 405 nm. Absorbance was plotted against time. Also, the rate of the enzyme activity was evaluated by an assay using methanol without an inhibitor. Any increase in the absorbance due to the spontaneous hydrolysis of substrate was corrected by subtracting the reaction rate before adding the enzyme from the rate after adding the enzyme. Inhibition percentage was obtained by comparing the rates of the sample to the blank (MeOH). Galantamine was used as the positive control.

2.6. Molecular modelling studies

Crystalline X-ray structures of the human AChE complex with E2020 have been obtained from the Protein Data Bank (PDB ID: 1EVE) (Abbas-Mohammadi et al., 2020). All heteroatoms were removed for preparing protein structures for docking, and Kollmann charges were assigned using the Protein Preparation Wizard using Schrodinger drug discovery suite (Schrödinger, Inc., New York, NY). The protein structure is minimized to relieve steric clashes using the OPLS3 force field (Optimized Potentials for Liquid Simulations 3). The minimization was terminated when the root-mean-square deviation (RMSD) reached a maximum value of 0.3 A°. Three-dimensional structural models of the test compounds were built using ChemBio-Draw V14 (Cambridge Soft, Cambridge, MA, USA) and saved in SDF format. The 3D structure of compounds was optimized using the Ligprep module in the Maestro 10.2 to generate all possible conformation at a physiological pH range of 7 ± 2. The grid box generation was performed using default glide settings with a general size of 10×10×10 A° for docking. In this work, standard precision (SP) docking protocol used for molecular modeling. The van der Waals scale factor of 0.8 is used for the protein atoms with partial charges less than or equal to 0.25. The Qikprop application was used to obtain the ADMET properties.

3. Results and Discussion

The isolation and purification of hexane extract from the aerial parts of *T. nephrophyllum* led to the identification of three coumarins, one steroid, and triterpene. The structures of the isolated compounds were elucidated by applying 1D and 2D NMR spectroscopy and compared with literature data. The isolated compounds were 5-geranyloxycoumarin (**1**) (Iranshahi et al., 2012), isobergapten (**2**), pimpinellin (**3**) (Ozek et al., 2019), β-sitosterol (**4**) and dammara-20,23-dien-3β,25-diol (**5**) (Révész et al., 1999) (Fig. 1). The complete NMR data of the isolated compounds are presented in Table 1 and Table 2. Compound **2** showed the typical coumarin ^{1}H-NMR pattern in the downfield region at δ_H 7.68 (d, 9.8 Hz) and 5.84 (d, 98 Hz), which corresponds to the C-3 and C-4 protons of the coumarin moiety. Also, the presence of the benzofuran ring has been confirmed by signals at δ_H 7.1 (d, 2.2 Hz), 6.55 (d, 2.2 Hz), and 6.41 (d, 2.2 Hz). The ^{1}H-NMR at δ_H 3.95 (s, CH_3) is attributed to the presence of the methoxy group. Comparing these data with literature value confirmed the structure of isobergapten (**2**). The inspection of NMR data for compound **3** showed missing of a signal at δ_H 6.41 and the presence of additional singlet (3H) signal at δ_H 3.95, which corresponds to the methoxy group. Therefore, compound **3** was identified as pimpinellin. The ^{1}H-NMR spectrum β-sitosterol (white sediment : 30 mg) showed the presence of 6 high-intensity peaks indicating the presence of six methyl groups at δ 0.65, 0.83, 0.85, 0.87, 0.94, and 1.01 ppm. A broad triplet at δ 5.21 corresponding to H-6 olefinic proton and a multiple at 3.57 corresponding to H-3 proton are detectable. Furthermore, the rest of the protons are observed in the high field region between 0.65 and 2.0 ppm. Previously, this compound has been characterized by the presence of δ 5.31 (1H, m H6) and 3.51 (1H, m H3) in the ^{1}H NMR spectrum. Nowadays, humans face a variety of persistent diseases. Undoubtedly, medicinal and herbal plants, which often involve many valuable bioactive compounds relating to different classes of natural products, can be considered as one of the best strategies to combat these illnesses (Nahar et al., 2021). For instance, some compounds belonging to different classes of metabolites such as limonoids, triterpenoids, coumarins, steroids, alkaloids, stilbenes, and phenolic compounds, have been extracted from the genus *Ekebergia* (Meliaceae). Some of these compounds displayed various bioactivities, including antiplasmodial, antimicrobial, antiproliferative, or uterotonic activities (Mouthe Kemayou et al., 2021). The genus *Haplophyllum* Juss is another valuable source of precious natural compounds, *e.g.*, terpenoids, coumarins, alkaloids, lignans, flavonoids, and organic acids. These natural products represented some remarkable antimicrobial, antifungal, anti-inflammatory, anticancer, cytotoxic, antileishmanial, and antialgal effects as well as promising remedial therapeutic properties (Mohammadhosseini et al., 2021; Mouthe Kemayou et al., 2021). Moreover, various pharmacological activities, including antibacterial, anti-hyperglycemic, anti-inflammatory, anti-pyretic, anti-diuretic, anti-larvicidal, anti-stress, and estrogenic, have been reported from *Cheilocostus speciosus* (J.Koenig) C.D.Specht (Hussain and Mazumder, 2021). Coumarins, a class of organic compounds, consist of a 1,2-benzopyrone ring system as a basic parent scaffold (Venkata Sairam et al., 2016). Coumarins have attracted extensive attention from researchers because of their abundant sources, easy synthesis, and various pharmacological activities. Coumarins showed a wide range of pharmacological activities, including anti-tumor (Wu et al., 2020), antihypertensive (Razavi et al.,

2015), anti-HIV (Xue et al., 2010), antihyperlipidemic (Iyer and Patil, 2014), anti-inflammatory (Bansal et al., 2013), analgesic, etc. (Zhu and Jiang, 2018). However, the relationships between their pharmacological effects and chemical structures have been proven, which are the basis of drug design (Iranshahi et al., 2009).

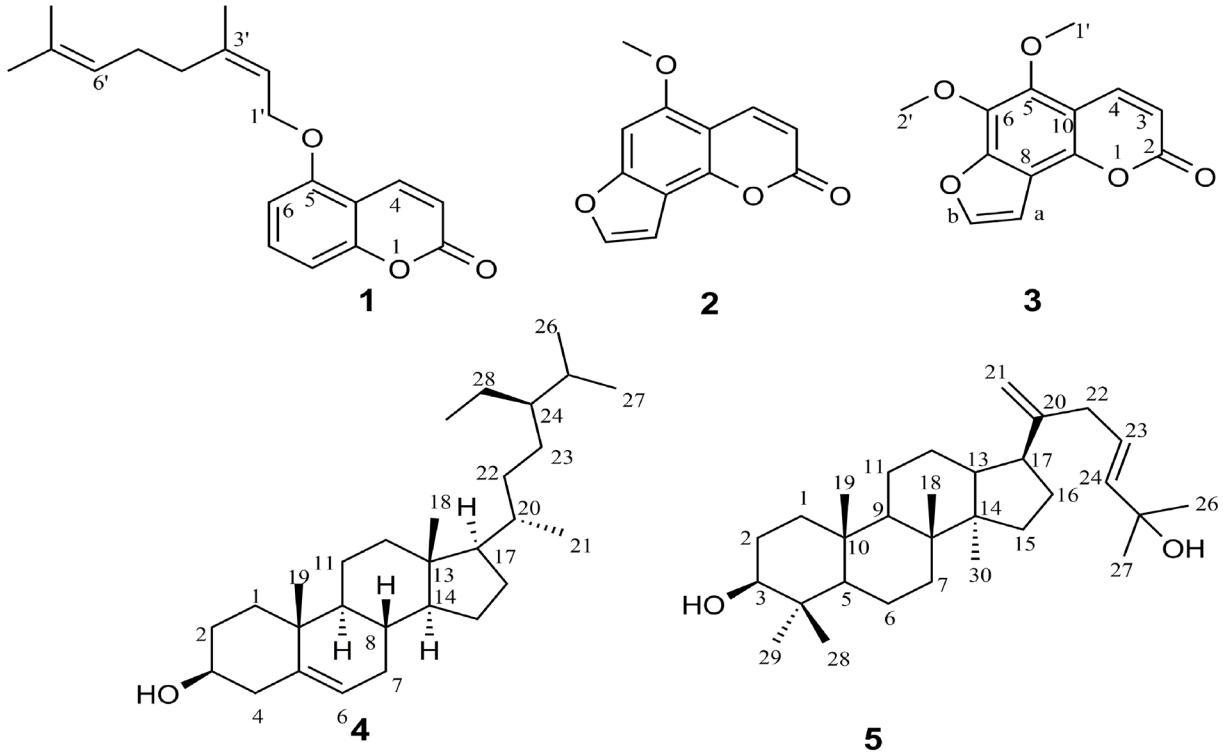

Fig. 1. Structures of the isolated compounds **1**-**5.**

Table 1
The ^{1}H, ^{13}C -NMR spectra of isolated coumarins **1**-**3** in $CDCl_3$.

Position	Compound 1		Compound 2		Compound 3	
	δ_H (mult *J* in Hz)	δ_C	δ_H (mult *J* in Hz)	δ_c	δ_H (mult *J* in Hz)	δ_c
2	-	161.0	-	160.9	-	160.8
3	6.25 (d, 9.5)	112.7	7.68 (d, 9.8)	139.6	7.98 (d, 9.8)	139.7
4	7.67 (d, 9.5)	143.4	5.84 (d, 9.8)	111.9	6.27 (d, 9.8)	113.6
5	-	162.1	-	154.3	-	135.3
6	6.85 (d,2.4)	101.3	6.41 (d, 2.2)	90.4	-	144.3
7	6.89 (dd, 8.6, 2.4)	113.1	-	158.2	-	149.8
8	7.40 (d, 8.6)	128.6	-	110	-	113.9
9	-	156.5	-	148.7	-	143.7
10	-	112.5	-	105.7	-	109.5
a	-	-	6.55 (d, 2.2)	103.9	6.99 (d, 2.1)	104.2
b	-	-	7.1 (d, 2.2)	144.1	7.57 (d, 2.1)	145.5
1′	4.65 (d, 6.5)	65.5	3.5 (s)	56.2	4.05 (s)	60.8
2′	5.51(td, 6.5, 1.1)	118.5	-	-	3.95 (s)	61.8
3′		141.7	-	-	-	-
3′a	1.81 (s)	16.5	-	-	-	-

Table 1 Continued

Position	Compound 1		Compound 2		Compound 3	
	δ_H (mult *J* in Hz)	δ_C	δ_H (mult *J* in Hz)	δ_c	δ_H (mult *J* in Hz)	δ_c
4′	2.13 (td, 12.1, 6.1)	39.3	-	-	-	-
5′	2.16 (td, 12.1, 6.1)	25.8	-	-	-	-
6′	5.13 (ddd, 6.7, 5.4, 1.1)	123.5	-	-	-	-
7′		131.6	-	-	-	-
7′a	1.71 (s)	25.0	-	-	-	-
8′	1.65 (s)	17.5	-	-	-	-

Table 2
The ^{1}H, ^{13}C-NMR spectra of isolated terpenoids **4**-**5** in $CDCl_3$.

Position	Compound 4		Compound 5	
	δ_H (mult *J* in Hz)	δ_c	δ_H (mult *J* in Hz)	δ_c
1	1.07 (m)	37.2	1.62 (m)	39.2
	1.87 (m)		0.86 (m)	
2	1.52 (m)	31.6	1.49 (m)	38.7
	1.182(m)		1.52 (m)	
3	3.57 (m)	72.3	3.14 (dd, 10.6)	78.5
4	2.25(m)	42.27	-	38.7
	2.29 (m)			
5	-	140.7	0.63 dd(12.5,1.3)	55.5
6	5.21 (lH, d, *J*=4.7)	119.7	1.63 (m)	17.8
			1.43 (m)	
7	1.75(m)	31.8	1.19 (m)	36.4
	2.04 (m)		1.48 (m)	
8	1.47 (m)	31.8	-	34.7
9	0.96 (m)	50.1	1.2 (m)	50.7
10	-	36.5	-	39.3
11	1.48 (m)	21.2	1.11 (m)	21
	1.53 (m)		1.42 (m)	
12	1.15 (m)	39.8	1.8 (m)	28.7
	1.98 (m)		1.03 (m)	
13	-	42.19	1.58 (m)	45
14	1.02 (m)	56.8	-	48.41
15	1.06 (m)	24.4	1.19 (m)	28.86
	1.55 (m)		1.74 (m)	
16	1.85 (m)	27.5	1.8 (m)	29
	1.72 (m)		1.32 (m)	
17	1.13 (m)	55.9	2.11 (m)	47.4
18	0.65 (s)	12.04	0.89 (s)	15.76
19	1.01 (s)	24.1	0.77 (s)	16.3
20	1.37 (m)	36.1	-	151.8
21	0.94 (d)	19.98	4.79 (s)	109.2
			4.71 (s)	

Table 2 Continued

Position	Compound 4		Compound 5	
	δ_H (mult *J* in Hz)	δ_c	δ_H (mult *J* in Hz)	δ_c
22	1.48 (m)	33.9	2.57 (d, 7)	37.3
23	1.12(m)	26.0	5.58 (d, 16)	125.7
24	0.98 (m)	45.8	5.72 (dt, 16.7)	139.1
25	1.68 (m)	29.1	-	69.8
26	0.83 (d, 6.3)	20.1	1.36 (s)	28.7
27	0.85 (d, 6.1)	19.8	1.36 (s)	28.7
28	1.20(m)	23.0	0.89 (s)	16.1
29	0.87 (t)	11.8	0.68 (s)	15.2
30	-	-	0.9 (s)	27.8

3.1. AChE inhibitory activity

The anti-AChE activity of isolated compounds was assessed *in vitro* by using the reported protocol. The extract showed inhibitory activity for AChE with an IC_{50} value of 159.5 µg/mL. All of the isolated compounds were evaluated in the *in vitro* assay. The obtained IC_{50} values of compounds are presented in Table 3 ranged between 0.208-0.796 µM to 172.1 µg/mL, compared with reference drug galantamine (0.005 µM). All compounds showed good inhibitory activity against AChE. Among the tested compounds, **3** and **5** with IC_{50} values of 0.208-0.231 µM µg/mL were the most potent compounds. In addition to the molecular docking evaluation, in this study, physiochemical properties of compounds are investigated by using AMET properties using the Lipinski rule of five (Ro5). These rules determined drug-like properties of compounds and containing hydrogen bond donor (HBD), hydrogen bond acceptor (HBA), molecular weight (MW), and the logarithm of the partition coefficient between water and 1-octanol (log P) (Shahriari et al., 2021). Furthermore, polar surface area (PSA) was added for completing Ro5. Based on these rules, drug molecules should have a molecular weight of 500 Da or less, a maximum of 5 HBDs or less, equal to or less than 10 HBAs, and log P equal to 5 or less. Lack of oral activity and bioavailability is more likely if two of these rules are not followed. Moreover, a compound with PSA equal to 140 A˚ or less will show a proper orally bioavailable drug. The docking simulation was performed to get insight into whether and how isolated compounds bind and inhibit the profile. The docking scores ranged between -7.7 to 6.3 kcal/mol (Table 3). The compounds **3** and **5** were the most active ones with the docking score of -7.7 and 7.5 kcal/mol, respectively. The interaction of compound **3** with the AChE enzyme represented in 2D and 3D models is displayed in Fig. 2. As seen, compound **3** carried out one hydrogen bond with residues HIP440 in the enzyme's backbone. Moreover, the benzene ring in furanocoumarin engages π-π stacking with Tyr121. Furthermore, the detail of the interaction of compound **5** with enzyme is displayed in Fig. 3. The compound **5** formed one hydrogen bond with residues GLH199 and several other interactions. From the results, it is demonstrated that the inhibitor is well-fitted in the active site. Analyzing Lipinski rules and ADMET properties of compounds such as MW, H-bond donors, H-bond acceptor (QPlogPo/w) and PSA revealed that the molecules follow these rules (Table 3). All factors mentioned were within the allowed range, indicating the high potential of ligands selected as a drug-type molecule.

Table 3
The acetylcholinesterase activities and binding energy values of enzyme and AMDET properties.

Compounds	LogP	MW	HBD	HBA	PSA	Rotatable bond	Experimental IC_{50} (µg/mL)	Experimental IC_{50} (µM)	Docking energy (kcal/mol)
1	4.2	298	0	3	47.1	6	122.1 ± 1.1	0.409 ± 0.004	-6.9
2	1.5	216	0	3	56.5	1	172.1 ± 2.1	0.796± 0.010	-6.3
3	1.5	246	0	4	63.3	2	51.2 ± 0.4	0.208± 0.002	-7.7
4	7.1	442	2	2	39.8	6	163.3 ± 1.5	0.369± 0.003	-6.3
5	7.6	414	1	1	22.4	7	95.8 ± 0.3	0.231± 0.001	-7.5
Galantamine	2	287	1	5	43.6	2	1.4 ± 0.2	0.005± 0.001	-8.8
Extract	-	-	-	-	-	-	159.5 ± 3.2	-	-

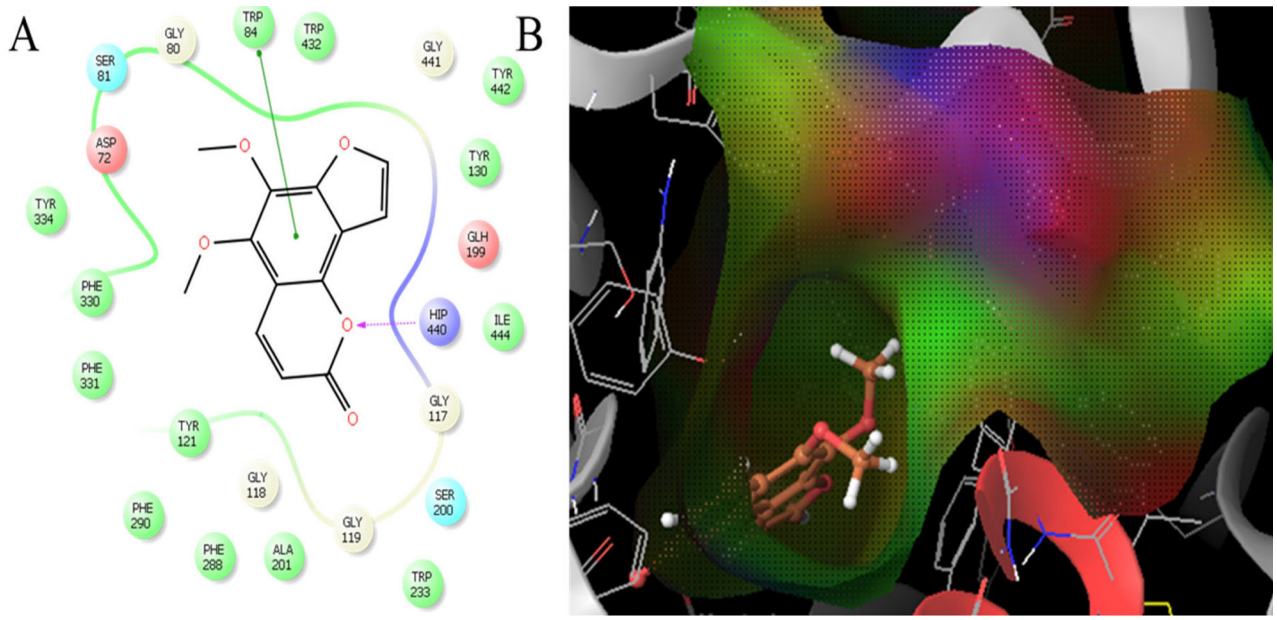

Fig. 2. Ligand-protein 2D (**A**) and 3D (**B**) interactions compound **3** with acetylcholinesterase enzyme and the position in the active site.

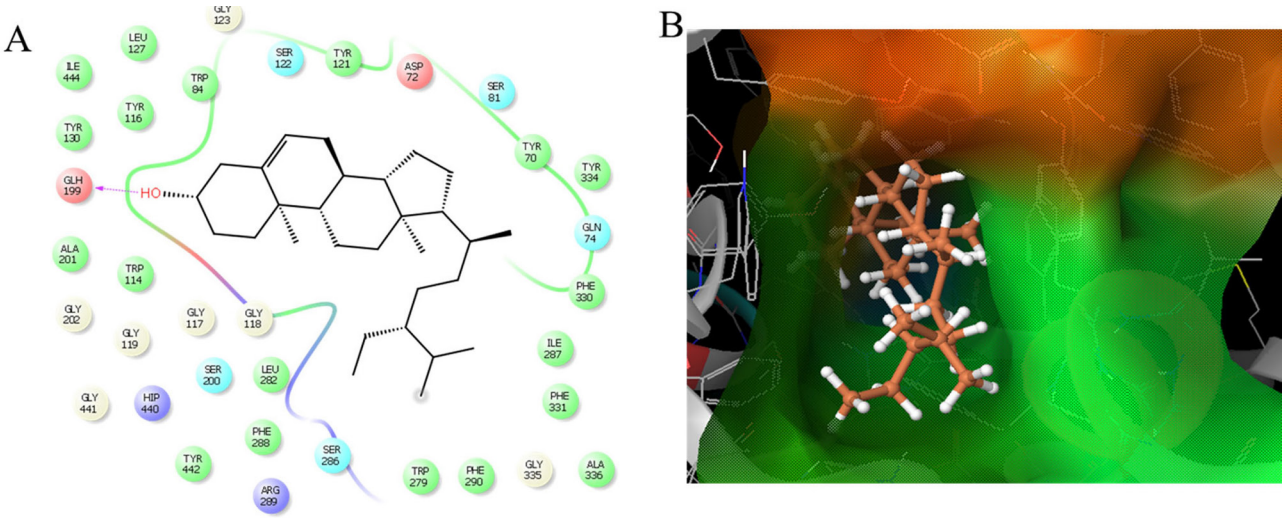

Fig. 3. Ligand-protein 2D (**A**) and 3D (**B**) interactions compound **4** with acetylcholinesterase enzyme and the position in the active site.

4. Concluding remarks

In this study, the phytochemical investigation of nonvolatile compounds from hexane extract of the aerial parts of *T. nephrophyllum* was investigated for the first time. Experimental and molecular docking methods subjected for evaluation of acetylcholinesterase inhibitory activity of extract and isolated compounds. Pimpinellin (**3**) showed the best acetylcholinesterase inhibitory with an IC_{50} value of 51.2 µg/mL and a docking score of -7.5 kcal/mol. Molecular docking analysis showed good agreement with experimental results.

Conflict of interest

The authors declare that there is no conflict of interest.

Acknowledgments

The authors wish to thank to Shahid Beheshti University Research Council for funding this project.

References

Abbas-Mohammadi, M., Moridi Farimani, M., Salehi, P., Ebrahimi, S.N., Sonboli, A., Kelso, C., Skropeta, D., 2020. Molecular networking based dereplication of AChE inhibitory compounds from the medicinal plant *Vincetoxicum funebre* (Boiss. & Kotschy). J. Biomol. Struct. Dyna. 1-10.

Ashrafi, H., Azadi, A., Mohammadi-Samani, S., Hamidi, M., 2020. New candidate delivery system for Alzheimer's disease: deferoxamine nanogels. Biointerface Res. Appl.

Chem. 10(6), 7106-7119.
Bansal, Y., Sethi, P., Bansal, G., 2013. Coumarin: a potential nucleus for anti-inflammatory molecules. Med. Chem. Res. 22(7), 3049-3060.
Brenner, G., 2000. Brenner and Stevens' Pharmacology E-Book. Philadelphia, PA.
Choudhary, M.I., 2001. Bioactive natural products as a potential source of new pharmacophores. A theory of memory. Pure Appl. Chem. 73(3), 555-560.
Ellman, G.L., Courtney, K.D., Andres, V., Featherstone, R.M., 1961. A new and rapid colorimetric determination of acetylcholinesterase activity. Biochem. Pharmacol. 7(2), 88-90.
Haghighatseir, N., Ashrafi, H., Rafiei, P., Azadi, A., 2020. Dexamethasone ameliorates Alzheimer's pathological condition via inhibiting Nf-kappa B and mTOR signaling pathways. Biointerface Res. Appl. Chem. 10(4), 5792-5796.
Hussain, M., Mazumder, T., 2021. A comprehensive review of pharmacological and toxicological properties of *Cheilocostus speciosus* (J. Koenig) CD Specht. Trends Phytochem. Res. 5(1), 1-12.
Iranshahi, M., Askari, M., Sahebkar, A., Hadjipavlou, L.D., 2009. Evaluation of antioxidant, anti-inflammatory and lipoxygenase inhibitory activities of the prenylated coumarin umbelliprenin. DARU J. Pharm. Sci. 99-103.
Iranshahi, M., Jabbari, A., Orafaie, A., Mehri, R., Zeraatkar, S., Ahmadi, T., Alimardani, M., Sadeghian, H., 2012. Synthesis and SAR studies of mono *O*-prenylated coumarins as potent 15-lipoxygenase inhibitors. Eur. J. Med. Chem. 57, 134-142.
Iyer, D., Patil, U., 2014. Evaluation of antihyperlipidemic and antitumor activities of isolated coumarins from *Salvadora indica*. Pharma. Biol. 52(1), 78-85.
Launer, L., Fratiglioni, L., Andersen, K., Breteler, M., Copeland, R., Dartigues, J., Lobo, A., Martinez-Lage, J., Soininen, H., Hofman, A., 1999. Regional Differences in the Incidence of Dementia in Europe-EURODEM Collaborative Analysis. Alzheimer's Disease and Related Disorders: Etiology, Pathogenesis and Therapeutics, 9-15.
Melzer, D., 1998. New drug treatment for Alzheimer's disease: lessons for healthcare policy. BMJ 316 (7133), 762-764.
Mohammadhosseini, M., Venditti, A., Frezza, C., Serafini, M., Bianco, A., Mahdavi, B., 2021. The genus *Haplophyllum* Juss.: Phytochemistry and bioactivities—A review. Molecules 26(15), 4664.
Mouthe Kemayou, G.P., Fotsing Kache, S., Dzouemo, L.C., M Happi, G., Fogue Kouam, S., Tchouankeu, J.C., 2021. Phytochemistry, traditional uses, and pharmacology of the genus *Ekebergia* (Meliaceae): A review. Trends Phytochem. Res. 5(3), 110-125.
Mukherjee, P.K., Kumar, V., Mal, M., Houghton, P.J., 2007. Acetylcholinesterase inhibitors from plants. Phytomedicine 14(4), 289-300.
Nahar, L., El-Seedi, H.R., Khalifa, S.A., Mohammadhosseini, M., Sarker, S.D., 2021. *Ruta* essential oils: composition and bioactivities. Molecules 26(16), 4766.
Oh, M., Houghton, P., Whang, W., Cho, J., 2004. Screening of Korean herbal medicines used to improve cognitive function for anti-cholinesterase activity. Phytomedicine 11(6), 544-548.
Ozek, G., Yur, S., Goger, F., Ozek, T., Andjelkovic, B., Godjevac, D., Sofrenic, I., Aneva, I., Todorova, M., Trendafilova, A., 2019. Furanocoumarin content, antioxidant activity, and inhibitory potential of *Heracleum verticillatum*, *Heracleum sibiricum*, *Heracleum angustisectum*, and *Heracleum ternatum* eExtracts against enzymes involved in Alzheimer's disease and type II diabetes. Chem. Biodivers. 16(4), e1800672.
Razavi, B.M., Arasteh, E., Imenshahidi, M., Iranshahi, M., 2015. Antihypertensive effect of auraptene, a monoterpene coumarin from the genus *Citrus*, upon chronic administration. Iran J. Basic Med. Sci. 18(2), 153.
Rechinger KH. (1982) Flora Iranica, Apiaceae, No. 162, Akademische Druck- u.Verlagsanstal Graz-Austria, 502-506.
Révész, L., Hiestand, P., La Vecchia, L., Naef, R., Naegeli, H.U., Oberer, L., Roth, H.J., 1999. Isolation and synthesis of a novel immunosuppressive 17α-substituted dammarane from the flour of the Palmyrah palm (*Borassus flabellifer*). Bioorganic Med. Chem. Lett. 9(11), 1521-1526.
Schulz, V., 2003. Ginkgo extract or cholinesterase inhibitors in patients with dementia: what clinical trials and guidelines fail to consider. Phytomedicine 10, 74-79.
Shahriari, M., Nourmandipour, F., Norouzi, S., Nejad Ebrahimi, S., 2021. Investigation of inhibitory properties of triphenyl-LasR enzyme involved in the quorum sensing of *Pseudomonas aeruginosa* by molecular modeling. Trends Phytochem. Res. 5(3), 126-135.
Sonboli, A., Azizian, D., Yousefzadi, M., Kanani, M., Mehrabian, A., 2007. Volatile constituents and antimicrobial activity of the essential oil of *Tetrataenium lasiopetalum* (Apiaceae) from Iran. Flav. Fragr. J. 22(2), 119-122.
Venkata Sairam, K., M Gurupadayya, B., S Chandan, R., K Nagesha, D., Vishwanathan, B., 2016. A review on chemical profile of coumarins and their therapeutic role in the treatment of cancer. Curr. Drug Deliv. 13(2), 186-201.
Wu, Y., Xu, J., Liu, Y., Zeng, Y., Wu, G., 2020. A review on anti-tumor mechanisms of coumarins. Front. Oncol. 10, 2720.
Xue, H., Lu, X., Zheng, P., Liu, L., Han, C., Hu, J., Liu, Z., Ma, T., Li, Y., Wang, L., 2010. Highly suppressing wild-type HIV-1 and Y181C mutant HIV-1 strains by 10-chloromethyl-11-demethyl-12-oxo-calanolide A with druggable profile. J. Med. Chem. 53(3), 1397-1401.
Zhu, J.J., Jiang, J.G., 2018. Pharmacological and nutritional effects of natural coumarins and their structure–activity relationships. Mol. Nutr. Food Res. 62(14), 1701073.